ELSEVIER

Polymer 43 (2002) 3901–3908

polymer

www.elsevier.com/locate/polymer

Behaviour of mesogenic side group polyacrylates in dilute and semidilute regime

Fabiano V. Pereira, Aloir A. Merlo, Nádya P. da Silveira*

Instituto de Química, Universidade Federal do Rio Grande do Sul, Av. Bento Gonçalves, 9500, CEP: 91501-970 Porto Alegre, Brazil

Received 17 October 2001; received in revised form 9 January 2002; accepted 14 March 2002

Abstract

The solution behaviour of a new mesogenic side group polyacrylate in tetrahydrofuran and toluene has been investigated by static and dynamic light scattering. In the dilute regime the polymer behaves as typical polydisperse linear chains in good solvent and the dynamics is dominated by a single fast mode. Cluster formation was detected starting at a concentration around 50 g l^{-1}. It seems to be independent of the solvent as well as of polymer molecular weight. In the semidilute regime, the behaviour of the reduced osmotic modulus leads to the conclusion that repulsion between the chains is stronger than in linear macromolecules. The appearance of larger clusters was revealed above a characteristic concentration and is slightly dependent on the polyacrylate molecular weight. The dynamics was generally characterised by a fast mode related to the cooperative diffusion and by a slow mode associated with large clusters. The existence of a network of multiconnected clusters is envisaged with increasing solution concentration.

Keywords: Liquid crystalline side-chain polyacrylate; Light scattering; Photon correlation spectroscopy

1. Introduction

Polymers containing mesogenic side groups are known as liquid crystalline side-chain polymers due to their liquid crystalline bulk properties [1]. The combination of macromolecular characteristics and the time scale of their electro-optic properties appears promising for applications in modern optical display technology [2]. Accordingly, such materials have been thoroughly investigated in the bulk [1–6] but only a few studies regarding their solution properties can be found [7–12]. Since the solubility of these polymers in many common solvents can be taken as good, the understanding of the relationship between their structure and properties can be improved by investigations in solution. Besides the information on individual chain characteristics and solvent quality obtained in the dilute regime, knowledge of the solution properties in the semidilute regime and higher polymer concentrations is also of interest. In semidilute solutions containing macromolecules, different chain architectures show characteristic deviations in the principal parameters analysed, such as the osmotic modulus, molecular weight dependence of the overlap concentration and aggregation process or cluster formation [12,13].

The aim of this work is therefore to study the solution properties of a new thermotropic liquid crystalline side chain polyacrylate containing 4′-*n*-alcoxyphenyl 4′-[1-(propenoyloxy)butyloxy]benzoate as mesogenic group [14]. It is attached to the polymer backbone by means of a spacer of length four methylene units, as represented in Fig. 1. After synthesis, investigation of the homologous series by polarisation microscopy revealed thermotropic behaviour, characterised by smectic phases [14]. In the present study, liquid crystalline polyacrylates with two different molecular weights have been investigated by means of polarised and depolarised static light scattering (SLS) as well as photon correlation spectroscopy (PCS). The solutions were prepared in two solvents, toluene and tetrahydrofuran (THF), since the solvent influence on the semidilute solution structure is not clear. The dilute and semidilute regimes were covered.

Comparison of the data obtained by the different techniques establishes the characteristic chain behaviour of the side chain polyacrylates in solution. The results are compared with those published for similar systems [3,12] and contribute to a better understanding of the solution behaviour of side chain liquid crystalline polymers, which present mesophase behaviour in the bulk.

* Corresponding author. Present address: Laboratoire de Spectrométrie Physique—CERMO CNRS UMR5588, Université Joseph Fourier de Grenoble, B.P.87, F-38402 St Martin d'Hères cedex, France. Tel.: +33-476-63-55-85; fax: +33-476-63-54-95.

E-mail address: nadya@iq.ufrgs.br (N.P. da Silveira).

0032-3861/02/$ - see front matter
PII: S0032-3861(02)00210-0

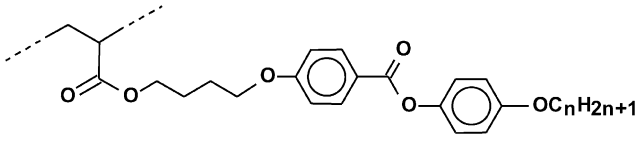

Fig. 1. Chemical formula of the repeating units of the investigated PLC. n is the number of carbons.

2. Experimental

The synthesis of the investigated liquid crystalline side-chain polyacrylates was performed as described in the literature [14]. Free radical polymerisation with AIBN as the radical initiator was performed in toluene. The chemical formula of the repeating units is given in Fig. 1 with n the number of carbon atoms on the flexible functional tail.

Table 1 lists the principal characteristics of the studied samples named PLC1 and PLC2. The refractive index increment dn/dc was measured with a modified Abbe refractometer at room temperature (20 °C). The solutions in THF and toluene were filtered through 0.2 μm pore diameter Millipore membranes into dust-free cells. The viscosity values of THF and toluene, 0.55 and 0.59 mPa s, respectively, were taken as published [15]. The highest concentrations, starting from 90 g l^{-1}, were obtained by evaporating previously filtered dilute solutions, inside a laminar flow box. The sample concentration was then determined from the weight difference. Light scattering experiments were performed on a Brookhaven instruments standard setup (BI-200M goniometer, BI-9000AT digital correlator) with a He–Ne laser ($\lambda = 632.8$ nm) as light source. The scattering volume was minimised using a 0.4 mm aperture and an interference filter was used before detecting the signal on the photomultiplier. The time correlation functions were measured in the multi-τ mode using 224 channels. The sample cell was placed in the index-matching liquid decahydronaphthalene (decalin, Aldrich) and the measurements were performed in the angular range 25–150° in steps of 5 or 10°. In order to measure the depolarised component of the scattered light, a high-quality Glan–Thomson prism having an extinction ratio better than 10^{-7} was used. The VH alignment was checked with CCl_4 and by measuring the depolarisation ratio of benzene at $\theta = 90°$.

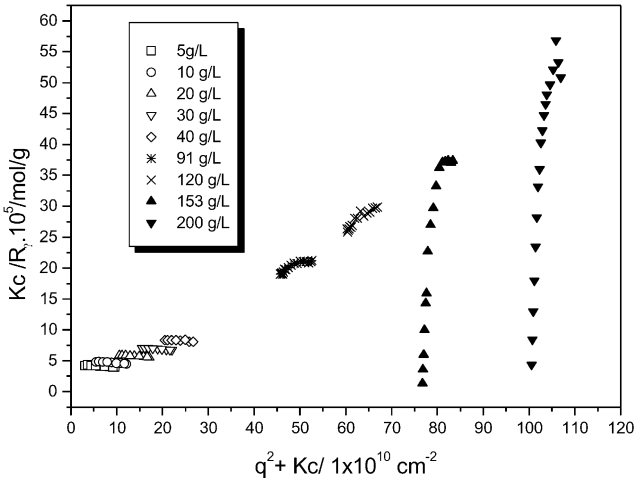

Fig. 2. Zimm plot of PLC1 in THF.

Table 1
Weight averaged molecular weight, M_w, obtained by SEC, number of carbons of the terminal tail, n, and refractive index increments, dn/dc, of PLC1 and PLC2 in THF and toluene

	M_w (g mol^{-1})	M_w/M_n	n	dn/dc (mL g^{-1})	
				THF	Toluene
PLC1	19,500	1.53	10	0.126	0.045
PLC2	48,100	3.16	10	0.126	0.045

3. Results and discussion

3.1. Static light scattering

3.1.1. Polymer characterisation

In SLS the data were obtained according to the simplified Zimm procedure [8], where the intensity of the scattered light is related to the weight average molecular weight, M_w, the second virial coefficient, A_2, and the radius of gyration, R_g, through the standard relation:

$$\frac{Kc}{R(\theta,c)} = \left[\frac{1}{M_w}\right]\left[1 + \frac{(R_g q)^2}{3}\right] + 2A_2 c. \quad (1)$$

In Eq. (1), $K = 4\pi^2 n^2 (\mathrm{d}n/\mathrm{d}c)^2/(N_A \lambda_0^4)$ is the optical contrast factor and q is the magnitude of the scattering vector $|\mathbf{q}| = (4\pi n/\lambda_0)\sin(\theta/2)$, with N_A, n, and λ_0 being Avogadro's number, the refractive index of the solvent and the wavelength of the light in vacuo, respectively. R_θ is the excess absolute time-averaged light scattering intensity (excess Rayleigh ratio). In order to obtain R_θ, the solvent scattered intensity is subtracted from the polymer solution intensity. In this work, the excess Rayleigh ratio of the solvent toluene (14×10^{-6} cm^{-1}) [16] was taken as reference. To extract the macromolecular parameters, measurements were extrapolated to infinite dilution ($c \to 0$) and zero angle scattering ($q \to 0$).

A typical Zimm plot obtained with PLC1 in THF is shown in Fig. 2. The results of the Zimm analysis performed on PLC1 and PLC2 in THF are listed in Table 2. Solutions with $c < 50$ g l^{-1} were taken into account.

The critical concentration $c^* = (A_2 M_w)^{-1}$, provides a good thermodynamic definition of the coil overlap concentration. A significant difference between values of M_w obtained by SLS and those obtained by SEC (Table 1) can be observed. Similar results were found by Burchard et al. [10] in a study of end-on/side-on polyacrylates. The discrepancy is due to the fact that SEC is based on a standard reference polymer whose structure is quite different from

Table 2
Results from SLS of PLC1 and PLC2 in THF and toluene

	THF				Toluene			
	M_w (g mol^{-1})	A_2 (mol cm^3 g^{-2})	R_g (nm)	c^* (g l^{-1})	M_w (g mol^{-1})	A_2 (mol cm^3 g^{-2})	R_g (nm)	c^* (g l^{-1})
PLC1	30,600	3.9×10^{-4}	–	83	39,500	2.3×10^{-4}	–	108
PLC2	108,000	2.1×10^{-4}	12.6	45	111,000	9.3×10^{-5}	10.5	97

that of the side group polyacrylates. SLS is thus the appropriate method for determining molecular weight of side chain liquid crystalline polymers. Due to the small values of dn/dc for these polyacrylates in toluene (Table 1), the error in M_w is higher in this solvent.

The strong angular dependence observed for R_θ in Fig. 2, starting from $c \geq 150$ g l^{-1}, corresponds to an additional contribution to the total excess scattering produced by long-range heterogeneities. These grow with increasing PLC1 solution concentration. Such an effect was observed in both THF and toluene. For PLC2, with a higher M_w, the angular dependence begins at $c \geq 120$ g l^{-1} in the solvent THF. The heterogeneities are related to large clusters in solution [10,12], formed by a random association process. It has been suggested for similar systems [12], that cluster formation is principally due to the presence of lateral groups in different polymer chains. In fact, the motion of the polymer backbone is restricted due to the mesogenic groups and the dipolar interaction between different mesogens attached to different chains may allow a kind of alignment of the mesogenic moieties [14].

The concentration for cluster formation observed for PLC2 in this work is the same as that found by Richtering et al. [12] for similar polymers with 5.5×10^4 g mol$^{-1} \leq M_w \leq 1.9\times10^6$ g mol^{-1}, in THF. However, for $M_w \leq 5.0\times10^4$ g mol^{-1}, a molecular weight dependence was observed with the PLC1 sample in this work. Probably, the chain conformation of the lower molecular weight polymer facilitates the intersegmental association in solution.

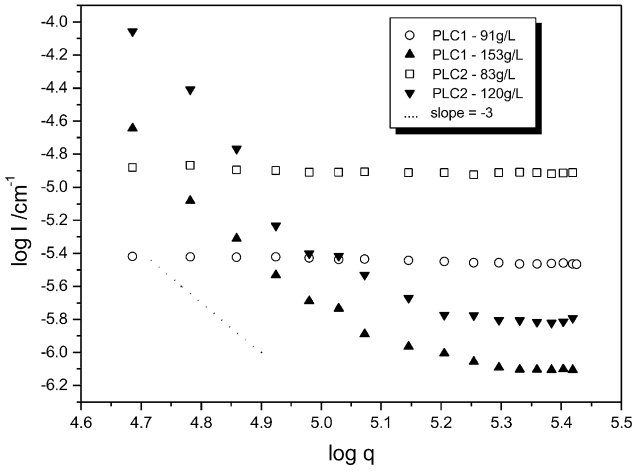

Fig. 3. Double-logarithmic plot of scattering intensity of PLC1 and PLC2 in THF as a function of the scattering vector.

In addition, comparison of our data with those of Richtering et al. [12] allows the effect of the spacer length between the mesogenic side group and the polymer chain to be explored. In Ref. [12], a common cluster formation concentration was found for samples having the mesogenic group laterally attached to the polymer backbone via a long flexible spacer. For samples with the mesogenic group directly fixed to the backbone, cluster formation was observed only at concentrations above 200 g l^{-1}. In this way, the flexibility of the mesogens attached to the polymer chain seems to be greater than that of the terminal tail for the cluster formation. Thus the characteristic concentration for cluster formation seems to be independent of chain length for side group liquid crystalline polymers with $M_w > 5.0\times10^4$ g mol^{-1}, being dependent on the mesogen mobility. Since the flexible spacers are quite different from those investigated elsewhere [12] (four methylene groups in the PLC2 studied here compared to 11 methylene groups in Ref. [12]), no influence on the characteristic concentration for cluster formation can be attributed to the spacer length.

The A_2 values in Table 2 indicate that both solvents are good for the samples investigated in this work. They are in agreement with results published for similar systems in THF [10,12]. The second virial coefficient evaluated from THF and toluene solutions decreases with increasing polymer molecular weight and is smaller in toluene, revealing decreasing solubility in this solvent. For this reason, solutions of PLC2 in toluene could not be obtained for $c >$ 90 g l^{-1}.

Values of the radius of gyration $R_g$were also obtained for PLC2 (Table 2). Since the molecular weight of PLC1, about 3.5×10^4 g mol^{-1}, corresponds to the low M_w limit for light scattering measurements of R_g, it was not reported.

3.1.2. Cluster characterisation

For scattering particles of radius R_g in a range of q for which $qR_g > 1$, the scattered intensity can be represented as a function of the fractal dimension d of the particle [10,17,18]:

$$I(q) \propto q^{-d}. \quad (2)$$

By applying Eq. (2), information about the cluster structure could be obtained in this work. A double logarithmic plot of I as a function of q is shown in Fig. 3. Slopes close to -3

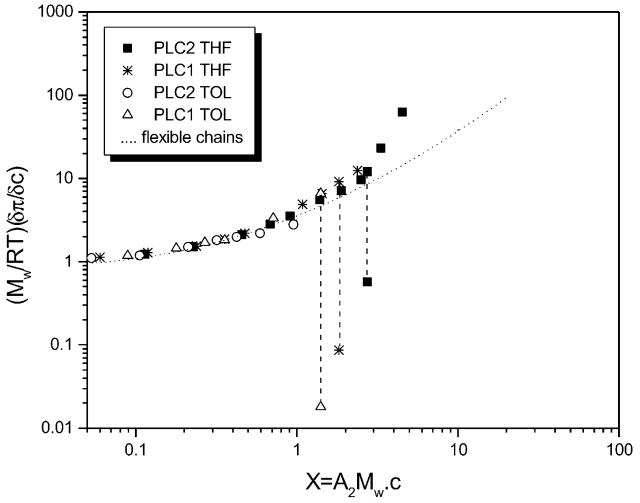

Fig. 4. Plot of the reduced osmotic modulus vs. the parameter $X = A_2 M_w c$ for PLC1 and PLC2 in THF and toluene.

were found for $c > 153\ \mathrm{g\,l^{-1}}$ in PLC1 and -4 for $c > 120\ \mathrm{g\,l^{-1}}$ in PLC2, indicating the presence of big isotropic clusters in solution. The increase in slope with increasing solution concentration suggests a network forming process of multiconnected clusters. PLC1 displayed the same behaviour in toluene, suggesting that the solvent has no influence on the solution structure for the low molecular weight side chain liquid crystal polymers. Unfortunately, owing to limited solubility, solutions of PLC2 in toluene with $c > 90\ \mathrm{g\,l^{-1}}$ could not be investigated.

The SLS intensity at $q \rightarrow 0$ is related to the osmotic modulus [12,13] through

$$\frac{Kc}{R_{\theta=0}} = \frac{1}{RT}\frac{\partial \pi}{\partial c}, \tag{3}$$

with π the osmotic pressure. Since this parameter is a measure of the repulsive forces among particles in a solvent, it can be applied to study the concentration effect on the solution structure.

To exhibit the universal behaviour of the investigated polymers, the reduced osmotic modulus $(M_w/RT)(\partial\pi/\partial c)$ can be plotted as a function of the thermodynamically normalised concentration $X \approx c/c^*$. Fig. 4 depicts such a plot for the samples in this work. For flexible linear chains of different molar mass a common curve can be seen. The theoretical curve given by renormalisation group theory [19] is depicted by the dotted line in Fig. 4. For dilute solutions, R_θ is linearly dependent on c, and extrapolation to $R_{\theta=0}$ is easily performed. Thus, for $X < 1$, the osmotic moduli are in agreement with the universal curve. However, for relatively high concentrations, when clusters are present, the solutions are no longer homogeneous and R_θ shows an angular dependence. For this reason, extrapolation to $R_{\theta=0}$ should be performed according to different q regions.

Thus, the discussion for $X > 1$ should take into consideration the high and low angles separately. These regions provide information about the solution properties and cluster formation, respectively. Values of R_θ extrapolated from high scattering angles to $R_{\theta=0}$ shows that the reduced osmotic modulus increases uniformly with concentration, in accordance with theory [19]. A deviation from the theoretical curve can be seen for $X > 1$. In this concentration range, the osmotic modulus is related to local properties of the entangled network and the observed behaviour can be attributed to a repulsion that is stronger than expected for linear macromolecules, owing to the presence of the lateral mesogenic groups. As expected, a stronger deviation is observed at high values of X in the solutions of PLC2, which has a higher molecular weight than PLC1. Similar behaviour is observed for the samples analysed by Richtering et al. [12], where a molecular weight dependence was seen for polymers having a flexible spacer between the polymer backbone and the mesogenic group.

The extrapolated value of the total excess scattering intensities at low angles appears as a component with a small osmotic modulus. These data are represented by the lower points on the dashed lines in Fig. 4. They indicate that the mass of the particles in solution increases due to cluster formation. The apparent change in the osmotic modulus is most drastic in the PLC1 solutions. In addition, owing to the lower solubility in toluene, this solvent has a major effect on the change. Unfortunately, since a quantitative extrapolation of the intensities in the low angle region to zero angle cannot be made from published work on similar systems [12], a comparison with our data cannot be made. However, our results show that cluster formation may be easier in the low molecular weight polymer solutions, since the excess scattering intensity associated with the appearance of clusters is stronger in this case. The excluded volume effect being smaller, the monomer–monomer inter-chain interaction can be expected to be facilitated.

A more detailed investigation of the cluster formation can be made by analysing the depolarised scattered light. Owing to liquid crystalline character of the side chain polymer, anisotropic components in the polarisability tensor are to be expected. This anisotropic or depolarised component may be sensitive to changes in the solution at short length scales, where cluster structures can be investigated. If the experiment is done with polarised incident light I_V, the polarised (I_{VV}) and depolarised (I_{VH}) light scattering components can be obtained. In order to characterise the anisotropic behaviour of the sample, usually the value of the depolarisation ratio ρ_V is employed, defined as [20]:

$$\rho = I_{VH}/I_{VV}. \tag{4}$$

In this work, the I_{VH} was obtained at a high scattering angle (135°) in order to allow the observation of the structural behaviour of the solution as a function of the polymer concentration.

Before discussing ρ_V we describe the expected behaviour of I_{VV} and I_{VH} as a function of solution concentration. First, in the dilute regime, a gradual increase of the polarised

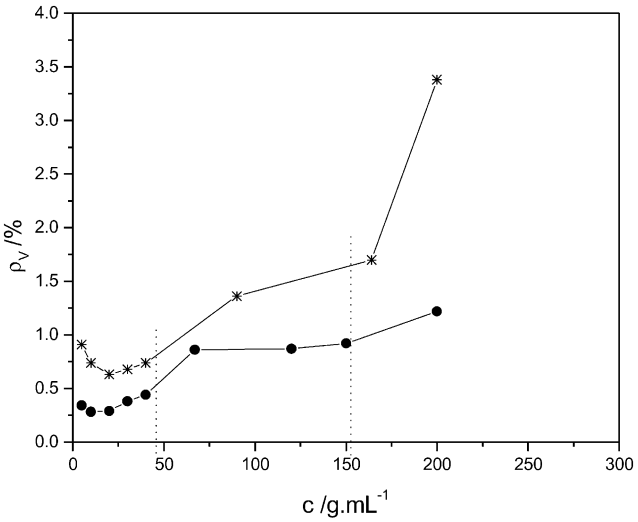

Fig. 5. Depolarisation ratio ρ_V as a function of concentration for PLC1 (✳) and PLC2 (●) in THF. The dashed lines are a guide for the eye, indicating the first appearance as well as the increase of the clusters in solution.

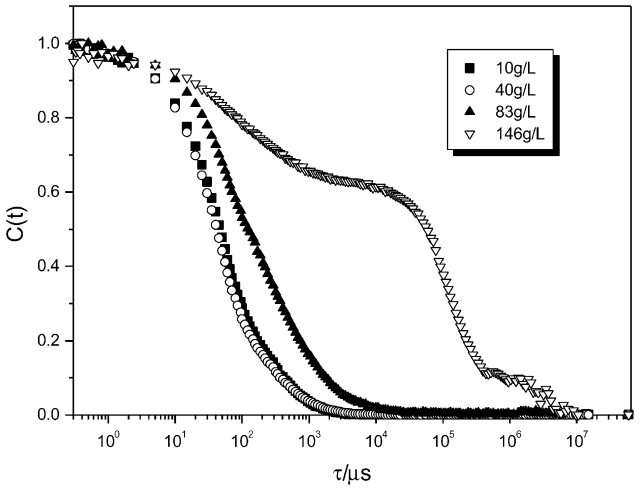

Fig. 6. Intensity correlation functions from PLC2 at different concentrations in THF at $\theta = 45°$.

scattered light should be observed with increasing polymer concentration, since I_{VV} is sensitive to the concentration fluctuations in solution. If clusters are formed, the polarised scattered intensity may increase proportionally to the cluster size, but no drastic increase should be seen at high angles. For I_{VH}, however, in addition to the polymer concentration, the mean optical anisotropy of the polymer chain influences the depolarised scattering intensity [21]: for highly flexible chains in sufficiently dilute solutions, the reduced optical anisotropy reaches an asymptotic value for $M_w \geq 2500$ g mol^{-1} [21]. Since the polyacrylates in the present work are less flexible and more extended in solution due to the side mesogenic groups, an increase of I_{VH} as a function of M_w may be observed. In addition, an increase in concentration may affect I_{VH} in a way that depends on the solution structure on the microscopic scale. Therefore, if clusters are formed due to specific mesogenic interactions on a short length scale, an anomalous increase in depolarised scattering will be observed, with an intensity that depends on the cluster size. Accordingly, the excess small angle scattering should change more drastically for PLC1 and a significant increase will be observed in I_{VV}. In contrast, for PLC2 a major increase should be observed in I_{VH}. Combined measurements of I_{VH} and I_{VV} can thus give interesting information about the cluster growth upon increasing the concentration.

Careful measurements performed in VV and VH geometry allowed ρ_V to be calculated in this work. In Fig. 5, a plot of ρ_V as a function of solution concentration is shown for the two polyacrylate liquid crystal (PLC) samples in THF. The small decrease of ρ_V occurring at the lowest concentrations ($c \ll 50$ g l^{-1}) is due to the non-linear increase of I_{VV}, which as expected, is more pronounced for PLC1. An increase in ρ_V starting from 50 g l^{-1} can be observed for both polymers, becoming more pronounced around 150 g l^{-1}, when big clusters are detected by SLS. The increase in ρ_V seems to depend on the polymer molecular weight for $c > 150$ g l^{-1}, with a stronger effect for PLC1, as expected. Similar behaviour of ρ_V was obtained for the solutions in toluene.

Inspection of Fig. 2 shows that a small excess Rayleigh ratio at small scattering angles can already be observed in the PLC1 Zimm plot for the intermediate solution concentrations (91 and 120 g l^{-1}). This effect may be a first sign of cluster formation.

From these results it can be concluded that cluster formation begins around 50 g l^{-1}, independently of the polymer molecular weight as well as of the solvent used. Starting from 150 g l^{-1} big clusters are present in solution. These two concentration regions are indicated by the vertical dashed lines in Fig. 5. As noted by other authors [10,12], the lack of dependence of cluster formation on chain overlap or polymer molecular weight and its dependence on solution concentration are further evidence that mesogenic groups may be responsible for cluster building.

3.2. Dynamic light scattering

3.2.1. Single chain diffusion

The time dependence of the intensity fluctuations in the scattered light was examined by PCS. Some examples of normalised intensity autocorrelation functions (CFs) are shown in Figs. 6 and 7, as a function of the solution concentration and detection angle, respectively. Up to a concentration of 83 g l^{-1} in PLC2, the CFs seem to be single exponential. The same behaviour was detected up to a concentration of 120 g l^{-1} in PLC1. The CFs were analysed by inverse Laplace transformation using the CONTIN program [22], which gives the amplitudes of the characteristic relaxation rates Γ ($= 1/\tau$) for each solution concentration. This analysis revealed, however, two relaxation modes, appearing above a sample concentration of

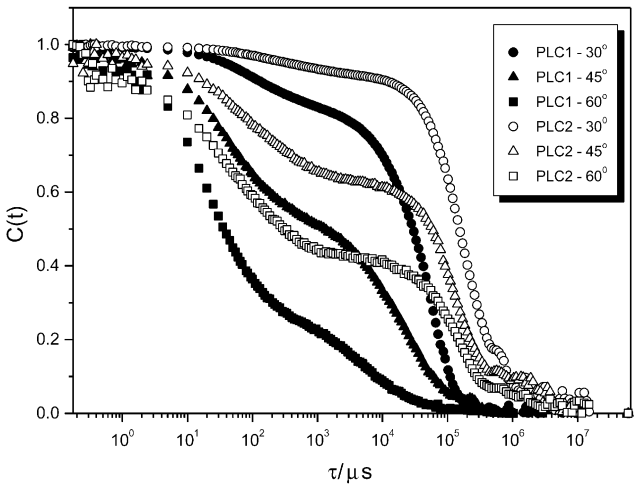

Fig. 7. Intensity correlation functions from PLC1 and PLC2 at different angles in THF (153 and 146 g l^{-1}, respectively).

approximately 50 g l^{-1}. The faster one always corresponds to the same dynamic process in this concentration range and is related to the diffusion dynamics of the single polyacrylate chain in solution. This mode is diffusive since Γ depends linearly on q^2. The q dependence of the slow process, however, which is not detectable at higher angles, could not be described satisfactorily. It is probably related to the dynamics of the incipient small clusters in solution.

The apparent translational diffusion coefficient D_{app} of the single polyacrylates chains was thus determined by using the values of Γ obtained according to Ref. [23]:

$$D_{app} = \frac{\Gamma}{q^2}. \tag{5}$$

Extrapolation to $q \rightarrow 0$ and $c \rightarrow 0$ gives the diffusion coefficient at infinite dilution D_0, which is related to the hydrodynamic radius R_h through the Stokes–Einstein relation [24]:

$$D_0 = \frac{k_B T}{6\pi\eta_0 R_h}, \tag{6}$$

with k_B the Boltzmann constant and η_0 the solvent viscosity.

In Table 3 are listed the values of D_0 and R_h obtained for PLC1 and PLC2 in THF and toluene. The diffusive dynamics of PLC1 is not affected by changing the solvent. The value of R_h for PLC2 in THF is similar to that determined elsewhere [12] for side group polyacrylates in the same solvent. PLC2 diffuses faster in the better solvent THF, as expected.

A comparison of R_g and R_h furnishes information on the coil conformation in solution through the parameter $\rho = R_g/R_h$ (Table 3). For the PLC2 sample in THF, ρ is found to be 2.1, a value that corresponds to polydispersed linear coils in a good solvent [25]. The value 1.6 obtained for the same sample in toluene may be attributed to a linear polymer coil with smaller dimensions, since solvation effects in toluene are less pronounced than in THF.

3.2.2. Cluster dynamics

For all the samples with concentrations above 150 g l^{-1} for PLC1 and 120 g l^{-1} for PLC2, at least two dynamic responses can be observed in the CFs (Figs. 6 and 7). The same behaviour was observed for PLC1 in toluene. Typical semidilute solutions of polymer in poor as well as good solvents show a slow dynamic mode, which depends on the coupling of the concentration fluctuations to the solution stress relaxation modes [26]. In this case, the slow mode may be q independent at large scattering angles. In this work, however, angular dependence was detected for the slow mode. Whereas the fast mode was related to the entanglement network, characteristic of a semidilute polymer solution [27], the dominant slow mode was associated with big clusters in solution. The existence of the clusters becomes obvious through the simultaneous appearance of small angle excess scattering in SLS and a slow motion in the PCS.

In this concentration range, CONTIN analysis revealed the presence of at least three mean relaxation times for small values of q. The middle one has been also observed in similar systems [12] and was explained as being related to the cluster decomposition. In the present work, however, the angular dependence of the central relaxation mode cannot be satisfactorily described.

Only for the samples with $c \approx 200$ g l^{-1} PLC1 and $c \approx 150$ g l^{-1} PLC2, did the values of Γ for the slow process not depend linearly on q^2. It can be imagined at this high polymer concentration, that the growth of multiconnected clusters could be responsible for such non-diffusive dynamics.

As can be seen in Fig. 6, the long time tail in the CFs becomes stronger with increasing polymer concentration. The strong angular dependence of the plateau height indicates that the clusters are large (Fig. 7). The relative intensity of the slow motion, determined by extrapolation of the plateau values to $q \rightarrow 0$, increases with the concentration

Table 3
Results from PCS of PLC1 and PLC2 in THF and toluene

	THF			Toluene		
	$D_0 \times 10^6$ (cm^2 s^{-1})	R_h (nm)	ρ	$D_0 \times 10^6$ (cm^2 s^{-1})	R_h (nm)	ρ
PLC1	1.2	3.4	–	1.2	3	–
PLC2	0.66	6.2	2.1	0.54	6.7	1.6

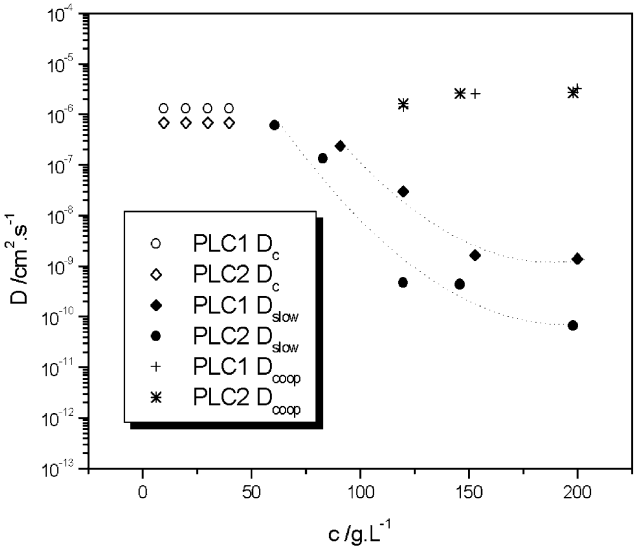

Fig. 8. Translational diffusion coefficients D_c, slow diffusion coefficient D_{slow}, and cooperative diffusion coefficient D_{coop}, as a function of polymer concentration.

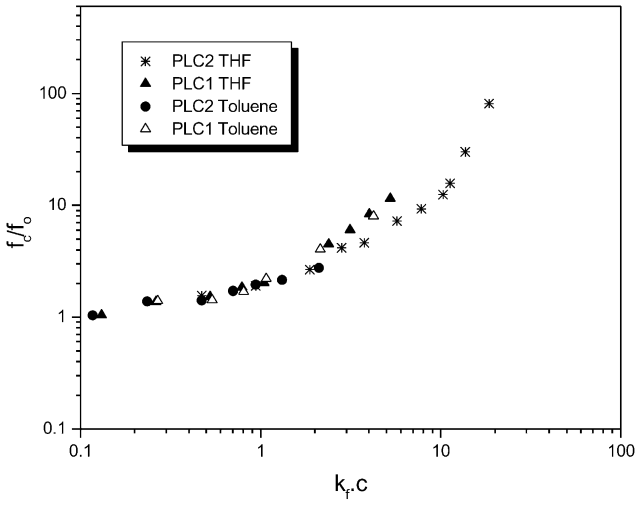

Fig. 9. Reduced friction coefficient as a function of $k_f c$ for PLC1 and PLC2 in THF and toluene.

and depends on the polymer molar mass. For the same concentration, the intensity scattered by the slow motion was higher for PLC2 than for PLC1.

In addition, the relaxation rates associated with the slow mode in the correlation functions yielded a slow diffusion coefficient D_{slow}, associated with the clusters. These results are depicted in Fig. 8 as a function of the molecular weight and solution concentration. This quantitative analysis suggests that the clusters are larger for the higher molar mass polymer, since the characteristic diffusion dynamics is slower. It is expected that with increasing polymer concentration the interaction between mesogenic side chains will increase leading to the formation of ordered domains. It seems probable therefore, that the observed large clusters correspond to such domains.

3.2.3. Cooperative diffusion

A quantitative analysis of the fast mode observed in the CFs for the samples with concentrations starting from 120 g l^{-1} was also performed in this work. Values for the cooperative diffusion coefficient D_{coop}, related to the entanglement network [27], as well as the hydrodynamic correlation length ξ_h were obtained from the Stokes–Einstein relation. They are listed in Table 4 for PLC1 and PLC2 in THF. Although the polymer concentration influences ξ_h, it seems to be independent of the polymer molecular mass.

As expected, D_{coop} increases with increasing c for all the samples. However, the exponent of the power law dependence is higher than the value of 0.77 [28] predicted for good solvents, and also higher than that for theta solvents (1), suggesting that the cooperative motion in this kind of system may be affected by motion of the mesogenic side chains in the solutions.

Fig. 8 shows the different diffusion coefficients obtained in this work as a function of sample concentration. According to the tendency indicated by dashed curves, cluster formation begins at about 50 g l^{-1}, for both polymers studied. No molecular weight dependence was observed for concentration range at which clustering begins.

In Fig. 8, the diffusion coefficient at finite concentration, D_c, can be related to the osmotic modulus by Ref. [12]

$$D_c = (k_B T/f_c)[(M_w/RT)(\partial\pi/\partial c)], \quad (7)$$

where f_c is the strongly concentration dependent friction coefficient. Thus, combining the results obtained by SLS and PCS, the friction coefficient f_c was calculated in this work. In the dilute concentration regime, however, the friction coefficient at infinite dilution f_0 can be obtained from the following relation [12]

$$f_c = f_0(1 + k_f c), \quad (8)$$

Table 4
Cooperative diffusion coefficient, D_{coop}, and hydrodynamic correlation length, ξ_h, for solution in THF, obtained by means of PCS

PLC1			PLC2		
c (g l^{-1})	$D_{coop} \times 10^6$ (cm^2 s^{-1})	ξ_h (nm)	c (g l^{-1})	$D_{coop} \times 10^6$ (cm^2 s^{-1})	ξ_h (nm)
120	1.4	2.8	120	1.6	2.4
153	2.5	1.6	146	2.6	1.5
200	3.1	1.2	198	2.7	1.5

which yields the value of the parameter k_f. Using this result, the reduced friction coefficient f_c/f_0 may be calculated and plotted as a function of the product $k_f c$ (Fig. 9).

It can be seen from Fig. 9 that the reduced friction for PLC1 displays no noticeable solvent dependence but exhibits a molecular weight dependence. The packing arrangement of the polymer segments causes more friction in PLC1 than in PLC2. Since PLC1 has lower molecular mass, it is likely that the chains are more extended.

4. Conclusions

The present results indicate that the side group PLC investigated behaves like a flexible linear chain with diffusive dynamics in dilute solution with organic solvents. Stronger repulsion than in linear chains was detected due to the presence of lateral mesogenic groups. Values of friction coefficients suggest, as expected, that the lower molecular weight chains may be more extended in solution. THF and toluene were found to be good solvents for the system, with THF the better one. The depolarised light scattering demonstrates that cluster formation starts at a characteristic concentration of 50 g l^{-1}, independent of chain molecular mass. In addition, according to their diffusion dynamics, the clusters grow larger with increasing concentration. The static scattering features show that clusters that form at concentrations about 120 g l^{-1} may be large, compact and homogeneous. The main results in the semidilute regime suggest that cluster formation is principally due to the intermolecular interaction between mesogenic groups of different polymer chains, as has been seen in similar systems. On increasing the polymer concentration, the fraction of polymer involved in the slow motion increases and the calculated correlation lengths tend to a constant value, indicating the existence of an entangled network of multiconnected clusters.

Acknowledgements

This work was kindly supported by the Brazilian Secretary for Science and Technology by the program PADCT. N.P.S. and F.V.P. acknowledge, respectively, a post-doctoral and a master fellowship from CAPES/Brazil. We are grateful to Dr Erik Geissler for helpful and stimulating discussions.

References

[1] Mc Ardle CD. Side chain liquid crystalline polymers. 1st ed. Glasgow: Blackie, 1988.
[2] Blackwood KM. Science 1996;273:909.
[3] Brostow W. Mechanical and thermophysical properties of polymer liquid crystals. 1st ed. London: Chapman & Hall, 1998. p. 124.
[4] Hamley IW, Davidson P, Gleeson AJ. Polymer 1999;40:3599.
[5] Yamada M, Itoh T, Nakagawa R, Hirao A, Nakahama SI, Watanabe J. Macromolecules 1999;32:282.
[6] Lam JWY, Kong Y, Dong Y, Chank KKL, Xu K, Tang BZ. Macromolecules 2000;33:5027.
[7] Springer J, Weigelt FW. Macromol Chem 1983;184:1489.
[8] Duran R, Strazielle C. Macromolecules 1987;20:2853.
[9] Ohm HG, Kirste RG, Oberthür RC. Makromol Chem 1988;189:1387.
[10] Richtering W, Schätzle J, Adams J, Burchard W. Colloid Polym Sci 1989;267:568.
[11] Mattoussi H, Ober R. Macromolecules 1990;23:1809.
[12] Richtering W, Gleim W, Burchard W. Macromolecules 1992;25: 3795.
[13] Bica CID, Burchard W, Stadler R. Eur Polym J 1997;33:1759.
[14] Magnago RF, Vollmer AF, Merlo AA, Mauller RS, Pereira FV, da Silveira NP. Polym Bull 1999;42:551.
[15] Lide DR, editor. Handbook of chemistry and physics 76th ed. New York: CRC Press, 1995. p. 8–64.
[16] Kaye W, Mc Daniel JB. Appl Opt 1974;13:1934.
[17] Bonczyc PA, Hall RJ. Langmuir 1991;7:1274.
[18] Lindner P, Zemb T. Neutron, X-ray and light scattering, 1st ed. Amsterdam: Elsevier, 1991. p. 318.
[19] Ohta T, Oono Y. Phys Lett A 1982;89:460.
[20] Berne BJ, Pecora R. Dynamic light scattering. 1st ed. New York: Wiley, 1976. p. 189.
[21] Pesce da Silveira N, Samios D, Strehle F, Dorfmüller Th. Macromol Chem Phys 1996;197:1945.
[22] Provencher SW. Comput Phys Commun 1982;27:213.
[23] Pecora R. Dynamic light scattering. 1st ed. New York: Plenum Press, 1985. p. 59.
[24] Pecora R. Dynamic light scattering. 1st ed. New York: Plenum Press, 1985. p. 97.
[25] Burchard W. Adv Polym Sci 1983;48:1.
[26] Wang CH, Zhang XQ. Macromolecules 1995;28:2288.
[27] Lindner P, Zemb T. Neutron, X-ray and light scattering. 1st ed. Amsterdam: Elsevier, 1991. p. 321.
[28] Koňák Č, Helmstedt M, Bansil R. Macromolecules 1997;30:4342.